Role of Phosphate in Initial Iron Deposition in Apoferritin†

Yonghong G. Cheng and N. Dennis Chasteen*

Department of Chemistry, University of New Hampshire, Durham, New Hampshire 03824

Received July 27, 1990; Revised Manuscript Received November 21, 1990

ABSTRACT: Ferritins from microorganisms to man are known to contain varying amounts of phosphate which has a pronounced effect on the structural and magnetic properties of their iron mineral cores. The present study was undertaken to gain insight into the role of phosphate in the early stages of iron accumulation by ferritin. The influence of phosphate on the initial deposition of iron in apoferritin (12 Fe/protein) was investigated by EPR, ^{57}Fe Mössbauer spectroscopy, and equilibrium dialysis. The results indicate that phosphate has a significant influence on iron deposition. The presence of 1 mM phosphate during reconstitution of ferritin from apoferritin, Fe(II), and O_2 accelerates the rate of oxidation of the iron 2-fold at pH 7.5. In the presence or absence of phosphate, the rate of oxidation at 0 °C follows simple first-order kinetics with respect to Fe(II) with half-lives of 1.5 ± 0.3 or 2.8 ± 0.2 min, respectively, consistent with a single pathway for iron oxidation when low levels of iron are added to the apoprotein. This pathway may involve a protein ferroxidase site where phosphate may bind iron(II), shifting its redox potential to a more negative value and thus facilitating its oxidation. Following oxidation, an intermediate mononuclear Fe(III)–protein complex is formed which exhibits a transient EPR signal at $g' = 4.3$. Phosphate accelerates the rate of decay of the signal by a factor of 3–4, producing EPR-silent oligonuclear or polynuclear Fe(III) clusters. In 0.5 mM P_i, the signal decays according to a single phase first-order process with a half-life near 1 min. In some experiments, a slow second phase, $t_{1/2} \geq 1$ h, was observed but accounted for 20% or less of the total loss in EPR intensity; this second phase probably corresponds to slow redistribution of iron on the protein. The mononuclear $g' = 4.3$ complex may arise from Fe(III) binding at a ferroxidase site or a nucleation site to which the Fe(III) has rapidly migrated following oxidation. Titration data suggest that a 3:1 P_i/Fe(III) complex is formed as the $g' = 4.3$ EPR signal decays. This complex may play a role in the migration of iron within the protein to form iron clusters, ultimately leading to formation of the core. The clusters can accommodate up to 0.38 ± 0.03 P_i/Fe as measured by equilibrium dialysis.

Ferritin, the iron storage protein, is widespread in plants, fungi, bacteria, and animals (Theil, 1987, 1989). In horse spleen ferritin, the iron is stored as a microcrystalline hydrous–ferric oxide–phosphate iron core, $(FeOOH)_8FeO{\cdot}H_2PO_4$, in the center of a protein shell with channels leading to the interior (Michaelis et al., 1943; Cranick & Hahn, 1944; Harrison, 1977; Clegg et al., 1980; Rice et al., 1983; Ford et al., 1984). Up to 4500 iron atoms may be stored in ferritin, but normally the protein averages half this amount (Treffry & Harrison, 1978). The hollow spherical protein shell, apoferritin, is composed of 24 subunits of similar or identical size, having an L subunit molecular weight of 19 824 (Heusterspreute & Crichton, 1981).

Ferritin can only be reconstituted in vitro from apoferritin, Fe(II), and O_2 or another suitable oxidant (Clegg et al., 1980; Macara et al., 1972; Treffry et al., 1979). A ferroxidase site has been recently identified on the H subunits of human liver ferritin (Lawson et al., 1989). While the protein itself is important in initiating core formation, once nucleation has begun, iron oxidation and deposition are thought to preferentially occur directly on the catalytic surface of the growing mineral (Macara et al., 1972; Clegg et al., 1980).

There is considerable interest in identifying the complexes of iron that are formed in the early stages of iron deposition in apoferritin. A mononuclear Fe(III) species exhibiting and EPR signal at $g' = 4.3$ has been identified as an initial iron(III)–apoferritin complex formed prior to significant core development (Rosenberg & Chasteen, 1982). A Fe(II)–Fe(III) mixed-valence dimer has also been observed (Chasteen et al., 1985; Hanna et al., 1991). Other intermediate oligomeric Fe(III) species have been recently identified by Mössbauer spectroscopy and EXAFS (Bauminger et al., 1989; Yang et al., 1987). While there appear to be several sites on the protein capable of binding iron, the indications are that iron redistributes to those sites where it is more thermodynamically stable and can form core (Chasteen & Theil, 1982; Wardeska et al., 1986; Harrison et al., 1986).

It is well-known that the iron cores of mammalian ferritins contain about 1–1.5% phosphorus as orthophosphate (Granick & Hahn, 1944; Mann et al., 1986). Approximately 60% of the phosphate appears to be located on readily accessible surface sites of the core (Granick & Hahn, 1944), while the remainder is more tightly bound, perhaps incorporated into stacking faults within the core crystallites (Treffry & Harrison, 1978). It has been suggested that the phosphate on the surface of the iron core interacts with the amino groups on the inner surface of the protein shell, acting as a bridging ligand for the binding of the iron core to the apoprotein (Imai et al., 1978; Harrison et al., 1974). However, phosphate is not essential for ferritin core formation in reconstituted ferritins as shown by Treffry and Harrison (1978) and Macara et al. (1972).

The high phosphate content of the more amorphous or disordered core structures of bacterial ferritins (Mann et al., 1987; Moore et al., 1986) may be the result of distribution of phosphate throughout the ferritin core complex (Mansour et al., 1985; Theil, 1983; Mann et al., 1986; Watt et al., 1986; Moore et al., 1986). EXAFS of reconstituted mammalian ferritin in the presence of phosphate indicates that this is the

† This work was supported by Grant GM20194 from the National Institute of General Medical Sciences.

* To whom correspondence should be addressed.

0006-2960/91/0430-2947$02.50/0

case (Rohrer et al., 1989). Such binding of the phosphate throughout the core is considered more stable than surface adsorption alone (Mann et al., 1986).

Investigations by high-resolution transmission electron microscopy (Mann et al., 1986) and Mössbauer spectroscopy (St. Pierre et al., 1986; Bauminger et al., 1980) suggest that high levels of phosphate result in a core resembling that of an amorphous hydrated iron phosphate mineral with a low degree of crystallinity rather than a hydrated iron oxide phase with a high degree of order (Webb & Macey, 1983; Treffry & Harrison, 1978; Williams et al., 1978). It has also been shown that the degree of the disorder of the core increases as the amount of phosphate present increases (Mann et al., 1986). Thus, high phosphate concentrations not only alter the composition of ferritin cores but also modify their structures as well.

An understanding of the role of phosphate in the iron core and in core formation is far from complete. In the present work, the role of phosphate in the initial phase of ferritin core formation from apoferritin, Fe(II), and oxygen was studied. The results show that phosphate accelerates Fe(II) oxidation, decreases the concentration of the intermediate $g' = 4.3$ mononuclear Fe(III)–apoferritin complex and hastens its decay, and becomes bound to the iron clusters so formed. The data are also consistent with iron(II) oxidation occurring via a single pathway, presumably involving a ferroxidase site on the protein.

Materials and Methods

All reagents were analytical reagent grade and used without further purification unless otherwise stated. Glassware was washed with 6 N HCl and rinsed thoroughly with doubly distilled and deionized water before use. Ferrous ammonium sulfate hexahydrate and sodium phosphate dihydrogen monohydrate were obtained from J. T. Baker Co., ferrozine and thioglycolic acid (TGA) were from Aldrich Chemical Co., Hepes [*N*-(2-hydroxyethyl)piperazine-*N*′-2-ethanesulfonic acid], Mops [3-(*N*-morpholino)propanesulfonic acid], and Mes [2-(*N*-morpholino)ethanesulfonic acid] were from Research Organics, Inc., sodium dithionite was from Fisher Scientific, sodium phosphate anhydrous was from Sigma Chemical Co., ammonium molybdate was from Mallinckrodt Chemical Works, and 57-Fe foil was from U.S. Services. Stock solutions used were 0.1 M ferrous ammonium sulfate in 0.01 M HCl and 0.1 M sodium phosphate (Na_2HPO_4/NaH_2PO_4) buffered at pH 7.5 or pH 6.2.

Apoferritin and Reconstituted Ferritin. Apoferritin was prepared by dialyzing cadmium-free horse spleen ferritin (Boehringer Mannheim) against thioglycolic acid (Chasteen et al., 1985). The concentration of apoferritin was determined spectrophotometrically with a Shimadzu Spectronic 200UV or Cary 219 spectrophotometer using a molar absorptivity of $E_{280nm} = 1.78 \times 10^4$ M^{-1} cm^{-1} $subunit^{-1}$ (Wardeska et al., 1986) on the basis of $E^{1\%}_{1cm} = 9.0$ (Stefanini et al., 1989) and a subunit molecular weight of 19824 (Heusterspreute & Crichton, 1981).

Analyses showed no detectable free phosphate in 42 μM apoferritin solutions to a detection limit of 0.8 μM. However, analyses performed on hydrolyzed apoferritin (vide infra) showed levels of 1.7 mmol of phosphate and 1.0 mmol of Fe/mmol of protein. Thus, trace amounts of phosphate and iron exist in the apoprotein prepared from ferritin.

Ferritin was reconstituted from apoferritin by the addition of Fe(II) stock solution to 42 μM apoferritin (1 mM subunit concentration) in 0.10 M Hepes (pH 7.5), 0.10 M Mops (pH 7.5), or 0.10 M Mes (pH 6.2) followed by air oxidation of the iron(II) through parafilm. The final concentration of Fe(II) was 0.5 mM, corresponding to 12 Fe/apoferritin. Except where indicated, the phosphate was added 20 min after addition of the Fe(II) with continued exposure to air.

EPR Spectra. X-band (9.2 GHz) EPR spectra were measured with a Varian E-4 spectrometer interfaced to a MINC-11/23 computer (Digital Equipment Corp.). Samples were maintained at 77 K with liquid nitrogen in a cavity dewar insert. In the kinetic studies, a single sample was repeatedly quick-frozen and quick-thawed to generate the points for each curve.

Hydrolysis of Apoferritin. A 0.50-mL aliquot of 126 μM apoferritin (3 mM subunit) or 0.50 mL of ultrafiltrate of apoferritin was added to 0.50 mL of 12 N HCl in a sealed glass tube under nitrogen and heated at 105 ± 4 °C for ~70 h. The acid was later removed in a vacuum desiccator over solid KOH until a dry residue was obtained (Devenyi & Gergely, 1974). After addition of 5.0 mL of deionized water, the residue was analyzed for phosphate or iron.

Iron Analyses. The stable purple complex ($\lambda_{max} = 562$ nm) formed between ferrozine and divalent iron was used in the determination of iron (Stookey, 1970) on hydrolyzed samples. The standard curve was linear from 0 to 45 μM Fe; 200 μL 1.8 mM dithionite was added to 200 μL of sample before the analysis was carried out. The final volume, including test reagents, was 5.0 mL. Iron concentrations were also measured by atomic absorption spectroscopy at 248 nm with an instrumentation Laboratory 951 aa/ae spectrophotometer. The range of linearity of the standard curve was 0–89 μM Fe.

Phosphate Analyses. The phosphate content of hydrolyzed samples was determined by the formation of a phosphomolybdate complex and its subsequent reduction to highly colored blue compounds (Strickland & Parsons, 1968). The analysis was carried out at 748 nm with the Cary 219 UV–visible spectrophotometer. The standard curve was linear from 0 to 25 μM P_i.

Equilibrium Dialyses. Equilibrium dialysis was carried out in 10-mL capped vials containing 5 mL of 1.25–2.50 μM P_i, labeled with ^{32}P, in 0.1 M Mops, pH 7.4. Each vial also contained a Spectra/Por molecular porous type 1 dialysis bag (molecular weight exclusion limit 6000–8000; Spectrum Medical Industries, Inc.) containing 1 mL of 20.8 μM apoferritin in the same phosphate buffer solution. Fe(II) was added to the protein solution to give a concentration of 250 μM Fe (12 Fe/protein) and allowed to air-oxidize. Measurement of the P_i content of the protein solution in the dialysis bag as a function of time showed no further changes in concentration after 24 h. After 48 h, the concentrations of P_i inside and outside of the bag and the protein concentration in the bag were measured for the various samples. ^{32}P counts were made in duplicate by using a Beckman LS 7000 scintillation counter and Aquosol-2 scintillation cocktail. Background corrections were made by running appropriate blanks.

Mössbauer Spectra. Mössbauer spectra were measured on a Ranger Scientific Mössbauer Model 1200 spectrometer equipped with a Cryo Industries exchange gas cryostat operating at liquid nitrogen temperature. $^{57}Fe(II)$ solution was prepared by the method of Bauminger et al. (1989). Samples of reconstituted ferritin with and without phosphate were prepared by the addition of 0.10 M $^{57}Fe(II)$ in 0.12 M H_2SO_4 to a solution of 84 μM apoferritin in 0.2 M Hepes, pH 7.5, with or without 1.0 mM phosphate. As controls, samples were also prepared by the addition of 0.10 M $^{57}Fe(II)$ stock solution to 0.1 M Hepes, pH 7.5, with or without 1 mM phosphate present. The samples were maintained at 0 °C in an ice/water

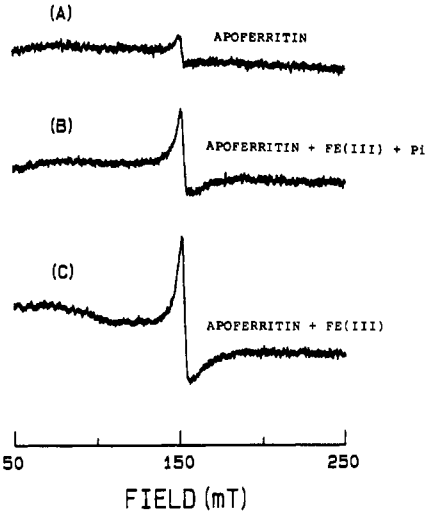

FIGURE 1: EPR spectra of (A) apoferritin, (B) reconstituted ferritin plus phosphate, and (C) reconstituted ferritin. Samples B and C were run 25 min after addition of Fe(II); in sample B, phosphate was added 20 min after the Fe(II). Conditions: 42 μM apoferritin, 0.5 mM Fe(II), and 0.5 mM phosphate in 0.1 M Hepes, pH 7.4. Instrument settings: modulation amplitude = 10 G, modulation frequency = 100 kHz, microwave power = 10 mW, microwave frequency = 9.37 GHz, scan range = 2000 G, scan time = 8 min, time constant = 0.3 s, and temperature = 77 K.

bath and, following addition of iron, were transferred at various times to Mössbauer cups and immediately frozen in liquid nitrogen.

Results

EPR Spectra at $g' = 4.3$ and Iron Analyses. EPR spectra for samples of apoferritin and reconstituted ferritin with phosphate and without phosphate are shown in Figure 1. The EPR signal at $g' = 4.3$ ($\sim$150 mT) is due to a Fe(III) mononuclear apoferritin complex (Rosenberg & Chasteen, 1982). A weak $g' = 4.3$ signal is also observed for the apoprotein (Figure 1A) due to residual iron in the protein ($\sim$1 Fe/protein, Materials and Methods). Fe(II) and Fe(III) solutions in Hepes buffer containing phosphate but no protein were found to be EPR-silent, demonstrating that the observed $g' = 4.3$ signal is from the protein.[1] Addition of P_i greatly attenuates the signal of the reconstituted ferritin (cf. Figure 1B,C).

Figure 2 shows the time course for the disappearance of the $g' = 4.3$ EPR signal plotted according to first-order kinetics. In the absence of P_i (Figure 2A), a two-phase first-order reaction is observed having rate constants and standard deviations of $k_1 = 16.3 \pm 2.5$ h^{-1} ($t_{1/2} = 2.6$ min) and $k_2 = 0.24 \pm 0.02$ h^{-1} ($t_{1/2} = 2.9$ h), corresponding to 38% and 62% of the total reduction in EPR intensity in the two phases, respectively.

In the presence of 0.5 mM phosphate, added 20 min after the addition of Fe(II),[2] a single-phase first-order reaction

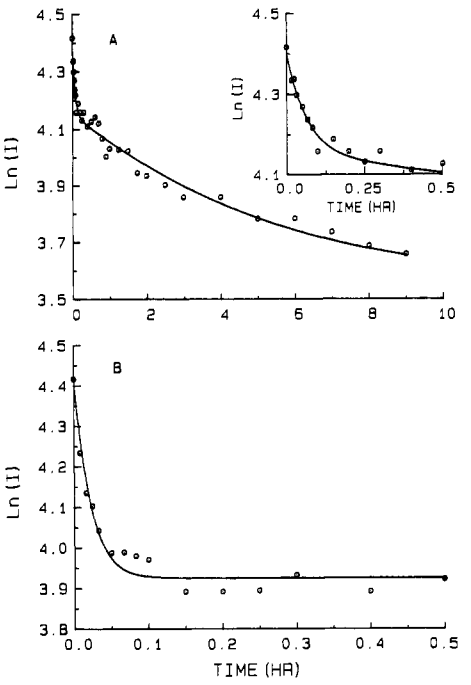

FIGURE 2: Plot of ln I vs time for the $g' = 4.3$ signal in the absence (A) and presence (B) of 0.5 mM phosphate. The solid line in (A) was calculated from a least-squares fit to the biphasic equation $\ln I = \ln \{(I_0 - I_\infty)[X \exp(-k_1 t) + (1 - X) \exp(-k_2 t)]\}$ where I, I_0, and I_∞ are the EPR amplitudes at time = t, 0, and ∞ h, respectively. The parameters from the least-squares fit are $X = 0.38 \pm 0.02$, $k_1 = 16.3 \pm 2.5$ h^{-1}, and $k_2 = 0.24 \pm 0.02$ h^{-1}. The solid line in (B) was calculated from a least-squares fit to the equation $\ln I = \ln [(I_0 - I_\infty) \exp(-kt)]$, giving $k = 50.9 \pm 4.9$ h^{-1}. Conditions: 42 μM apoferritin, 0.5 mM Fe(III) in 0.1 M Hepes (pH 7.4), with and without 0.5 mM P_i, 20 $\pm$ 1 °C.

having a rate constant of $k = 50.5 \pm 4.9$ h^{-1} ($t_{1/2} = 0.8$ min) is observed (Figure 2B). Thus, phosphate accelerates the rate of reduction of the EPR signal by approximately 3-fold. In some experiments performed under the same conditions, a slower second phase ($t_{1/2} \geq 1$ h) was observed in the presence of phosphate, but in all instances, this phase corresponded to less than 20%. In general, 0.5 mM phosphate caused an acceleration in rate by a factor of 3–4 and a total reduction in the $g' = 4.3$ signal of 80–90% compared to a 60–70% reduction observed in the absence of phosphate.[3,4]

EPR ($g' = 4.3$) time courses for reconstituted ferritins without phosphate at different temperatures and different pH values are shown in Figure 3A,B,C. At low pH (6.2, Figure 3C) or temperature (0 °C, Figure 3B), the rate of the reaction is sufficiently slowed that a maximum in the EPR signal of the mononuclear Fe(III)–apoferritin complex is observed, a result consistent with the proposal that this complex is an intermediate (Rosenberg & Chasteen, 1982). Higher temperatures and pH strongly favor disappearance of the complex (Figure 3A). Its maximum concentration is achieved in 6–8 min at 0 °C and pH 7.5 (Figure 3B) and in 20 s at 20 °C and pH 6.2 (Figure 3C).

The effect of molecular oxygen on the disappearance of the EPR signal was also investigated (Figure 3D). Increasing the

[1] Experiments were conducted to demonstrate that all the iron added during the reconstitution of ferritin, with or without phosphate present, becomes associated with the protein. Analysis of ultrafiltrates of reconstituted 42 μM ferritin containing 0.5 mM Fe, with or without 0.5 mM phosphate present, by the ferrozine method and by atomic absorption, 28 h after addition of iron, showed no iron at detection limits of $\sim$0.5 and 0.7 μM for the two methods, respectively. In contrast, the iron in 0.5 mM solutions of Fe(II), Fe(III) (in dilute HCl), and 1:1 Fe(III)/P_i in 0.1 M Hepes (pH 7.5) in the absence of protein freely passed through the ultrafiltration membrane.

[2] The addition of Fe(II) to a solution of apoferritin already containing phosphate resulted in the same kinetic curve as when P_i was added after the Fe(II). That is, after the point in time when both Fe(II) and P_i were present, the kinetic curves obtained were the same regardless of the order of addition.

[3] Hepes buffer has been recently shown to form a buffer radical species during Fe(II) oxidation by molecular oxygen (Grady et al., 1988). Since most of the present work had been completed with Hepes buffer, some kinetics experiments were also carried out using Mops buffer. Similar kinetic curves were obtained with either buffer (data not shown).

[4] The $g' = 1.87$ EPR signal of the Fe(II)–Fe(III) mixed-valence dimer observed near liquid helium temperatures is also attenuated by phosphate, but a detailed kinetic study was not undertaken.

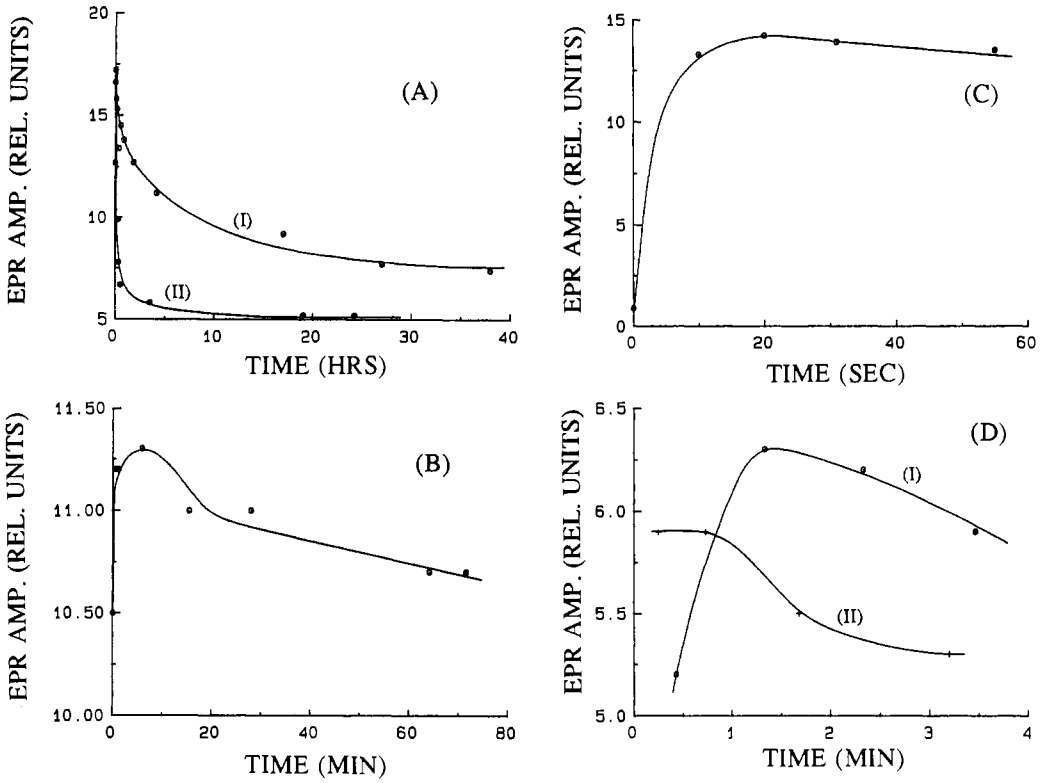

FIGURE 3: Temperature (A, B), pH (C), and oxygen (D) effects on the time course of the $g' = 4.3$ EPR signal. (A) 25 ± 1 °C (I); 40 ± 2 °C (II); pH 7.5; P_{O_2} = 0.2 atm. (B) 0 °C; pH 7.5; P_{O_2} = 0.2 atm. (C) 20 ± 3 °C; pH 6.2; P_{O_2} = 0.2 atm. (D) P_{O_2} = 0.2 atm (I); P_{O_2} = 1.0 atm (II); 20 ± 2 °C; pH 7.5. Conditions: 42 μM apoferritin; 0.5 mM Fe(II), 0.2 M Hepes, pH 7.5, except 0.1 M Mes, pH 6.2, was used in (C) and 2.5 mM Fe(II) was used in (D).

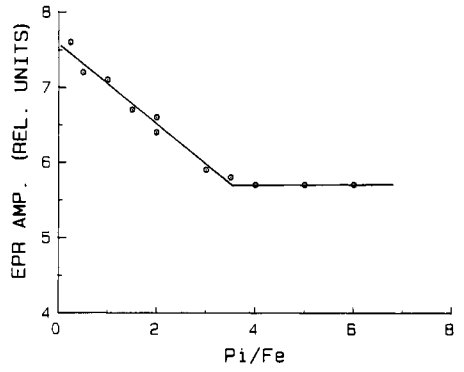

FIGURE 4: EPR intensities at $g' = 4.3$ of reconstituted ferritin vs the phosphate to iron ratio. P_i was added 20 min after the samples had been reconstituted. The EPR intensities were measured 20 min after addition of phosphate to reconstituted samples. Conditions: 42 μM apoferritin, 0.50 mM Fe(II), 0.10 M Hepes, pH 7.4, and different concentrations of phosphate, 20 ± 1 °C.

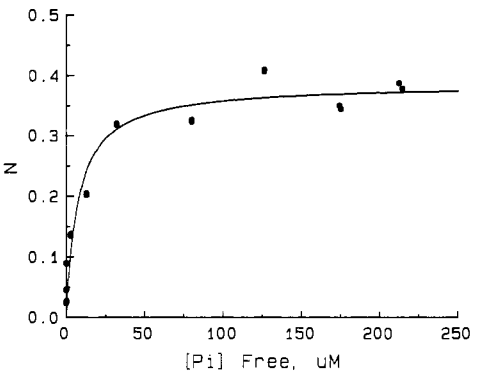

FIGURE 5: Phosphate binding to reconstituted apoferritin containing 12 Fe(III)/protein. N (=$[P_i]_{bound}/[Fe]$) versus $[P_i]_{free}$. Solid curve calculated from eq 1 in the text using $n = 0.38 \pm 0.03$ and $K = (1.3 \pm 0.5) \times 10^5\ M^{-1}$ (3 standard errors). Conditions: 20.8 μM apoferritin and 25 mM Fe(III) in 0.1 M Mops, pH 7.4, with varying P_i concentrations, 20 ± 1 °C.

oxygen tension from 0.2 atm (curve I) to 1.0 atm (curve II) decreases the maximum concentration of the mononuclear complex that is formed and accelerates its rate of disappearance. Such behavior would be anticipated if the mononuclear complex corresponds to a core nucleation species that disappears more rapidly in the presence of higher O_2 concentrations.

A plot of the EPR signal amplitude of reconstituted ferritin vs the phosphate to iron ratio is shown in Figure 4. In this experiment, the phosphate was added 20 min after addition of Fe(II) to the apoferritin. After another 20 min, the samples were frozen and their EPR spectra recorded. Figure 4 shows that a maximum reduction in the $g' = 4.3$ signal is obtained at a phosphate to iron ratio of 3.5. Five other experiments, where the EPR spectra were obtained from 5.5 min to 24 h after addition of P_i, gave an average P_i:Fe ratio of 3.1 ± 0.6.

These results suggest that the loss of the $g' = 4.3$ EPR signal is associated with the formation of a specific Fe(III)–phosphate complex having a P_i/Fe stoichiometry of ~3.0. This putative complex was not observed by EPR, presumably because it is present in such low concentrations or it is polynuclear and thus EPR-silent.

Equilibrium Dialysis. The binding of P_i to reconstituted ferritin containing a small amount of Fe (12 per molecule) was studied by equilibrium dialysis. Iron(II) was added aerobically to samples of apoferritin containing various amounts of phosphate and allowed to equilibrate for 48 h after which P_i analyses of solutions on both sides of the dialysis membrane were performed (Materials and Methods). Figure 5 shows a plot of N (=$[P_i]_{bound}/[Fe]_{total}$) versus the concentration of free P_i in solution. A saturation binding curve is obtained.

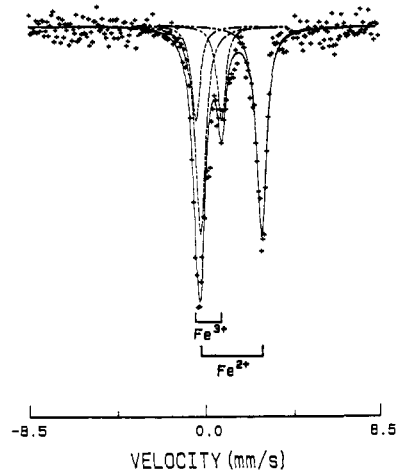

FIGURE 6: Typical Mössbauer spectrum of reconstituted ferritin. Solid line is computer fit to the entire spectrum. Dashed lines are individual peaks of the quadrupole doublets. Conditions: sample was held for 1.3 min at 0 °C before freezing. Concentrations: 84 μM apoferritin, 1.0 mM ^{57}Fe(II), and 0.1 M Hepes, pH 7.5. Instrument setting: velocity range = ±8.5 mm/s, triangular mode, 77 K.

The data were curve-fitted by nonlinear regression to eq 1 where K is the apparent association constant and n is the average stoichiometry of P_i binding to the iron (Scatchard et al., 1950; Fletcher et al., 1970). Values of $K = (1.3 \pm 0.5) \times 10^5\ M^{-1}$ and $n = 0.38 \pm 0.03$ (three standard errors) were obtained (Figure 5).

$$N = \frac{nK[P_i]_{free}}{1 + K[P_i]_{free}} \quad (1)$$

Mössbauer Spectra. Mössbauer spectra were measured on samples prepared by adding ^{57}Fe(II) solution to apoferritin with or without phosphate present followed by incubation for a period of time at 0 °C prior to quick-freezing at 77 K. Figure 6 shows a typical spectrum of the reconstituted ferritin shortly after introduction of the Fe(II). The spectrum shows the characteristic quadrupole doublets of divalent and trivalent iron. The spectra were computer-fitted to a pair of doublets having Lorentzian line shapes. The percentage of iron oxidized was calculated from the areas of the subspectra; the recoilless fractions for Fe(II) and Fe(III) were assumed to be the same. The Fe(III) Mössbauer parameters observed for the different samples as a function of time are summarized in Table I.

The percent iron(II) oxidized as a function of time (Figure 7) indicates that the presence of 1 mM phosphate during reconstitution significantly accelerates the rate of iron oxidation. A plot of log % Fe(II) vs time is linear, showing that the rate of disappearance of Fe(II) is first-order with rate constants of 0.45 ± 0.07 min^{-1} ($t_{1/2}$ = 1.5 ± 0.3 min) and 0.25 ± 0.02 min^{-1} ($t_{1/2}$ = 2.8 ± 0.2 min), in the presence and absence of phosphate, respectively. The presence of 1 mM phosphate accelerates the rate of Fe(II) oxidation 2-fold.

Discussion

Variation in phosphate content of the ferritin iron core alters not only the core structure (Theil, 1983; Rohrer et al., 1989) but also crystallinity (Mann et al., 1986, 1987), magnetic interactions (Williams et al., 1978), redox properties (Watt et al., 1985, 1986), and local environment of the iron in the core (Rohrer et al., 1989). The present study points toward a significant role for phosphate in the initial stages of core formation in ferritin.

Phosphate significantly accelerates the decay of the mononuclear $g' = 4.3$ Fe(III)–apoferritin complex (Figure 2).

Table I: Mössbauer Parameters[a]

		Fe(III)		Fe(II)	
sample	T_f	δ (mm/s)[b] (±0.02)	Δ (mm/s)[c] (±0.02)	δ (mm/s)[b] (±0.02)	Δ (mm/s)[c] (±0.02)
reconstituted ferritin with phosphate	1.6 min	0.31	1.10	1.50	2.67
	2.1 min	0.35	0.99	1.52	2.61
	2.6 min	0.35	0.99	1.54	2.66
	3.1 min	0.37	0.94	1.55	2.61
	3.6 min	0.41	0.89	1.55	2.60
	5.6 min	0.43	0.78	1.55[d]	2.71[d]
	24 h	0.50	0.68		
reconstituted ferritin without phosphate	1.3 min	0.28	1.22	1.36	2.98
	2.3 min	0.34	1.24	1.42	2.82
	4.3 min	0.37	1.08	1.50	2.68
	6.3 min	0.41	0.98	1.54	2.66
	9.3 min	0.46	0.86	1.48[d]	2.85[d]
	13.8 min	0.47	0.86	1.59[d]	2.49[d]
	24 h	0.46	0.72		
^{57}Fe + P_i + buffer	7.5	0.36	0.96	1.47	2.60
	14.5	0.39	0.89	1.49	2.56
^{57}Fe + buffer				1.38	3.22

[a] Conditions as in Figure 6. [b] δ, isomer shift relative to iron foil at room temperature. [c] Δ, quadrupole splitting. [d] The Fe(II) doublet accounts for less than 12% of the Mössbauer intensity of these samples, causing large uncertainties (±0.10 mm/s) in the values of δ and Δ.

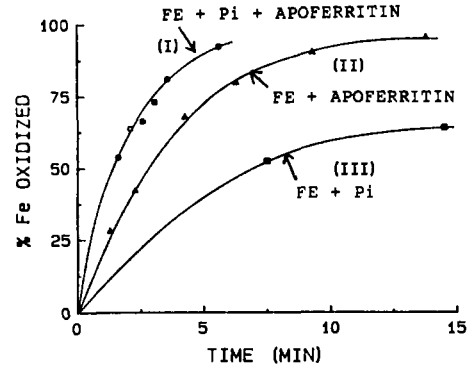

FIGURE 7: Time course of percentage of iron oxidized. Data calculated from fitted Mössbauer spectra. (I) ^{57}Fe-reconstituted ferritin with phosphate; (II) ^{57}Fe-reconstituted ferritin without phosphate; (III) ^{57}Fe with phosphate alone sample. Conditions: 84 μM apoferritin (I and II), 1.0 mM P_i (I and III), 1.0 mM ^{57}Fe(II) (I, II, and III), and 0.1 M Hepes, pH 7.5 (I, II, and III) and 0 °C. For (I), P_i was added 20 min *before* addition of ^{57}Fe(II). Instrument setting: velocity = ±8.5 mm/s, 77 K.

The decay of the complex occurs in two phases with half-lives of 2.6 min and 2.9 h in the absence of P_i. In the presence of 0.5 mM phosphate, the reaction proceeds essentially by a single phase (≥80%) having a half-life near 1 min. The slow second phase probably corresponds to a slow redistribution of iron(III) to the core. Changes over time in the ultraviolet spectrum of ferritin reconstituted with small amounts of iron have been attributed to similar phenomena (Treffry & Harrison, 1984). The Mössbauer data in Table I likewise indicate changes in the average environment of the iron(III) in the 24-h period following oxidation (vide infra), consistent with some rearrangement of the iron within the protein.

In addition to accelerating the rate of disappearance of the mononuclear Fe(III)–protein complex in each phase, the presence of phosphate increases from 38% to greater than 80% the percentage of the mononuclear iron(III) disappearing by the more rapid first phase. This multiple effect of phosphate significantly enhances the ability of the protein to convert the mononuclear $g' = 4.3$ Fe(III)–apoferritin complex to EPR-silent polynuclear clusters. The titration shown in Figure 4

suggests that a 3:1 P_i/Fe(III) complex is formed during this conversion. The formation of such a complex may be important in the translocation of iron between binding sites within ferritin.

A saturation value of 0.38 (1 P_i per 2.6 Fe) for the P_i:Fe ratio was achieved in the equilibrium dialysis experiment (Figure 5). In contrast, a much lower P_i:Fe ratio of 0.11 is typically found for native horse spleen ferritin with fully developed core (Granick & Hahn, 1944; Mann et al., 1986). Similarly, native human spleen ferritin has a P_i:Fe ratio of 0.13, but when the core is reconstituted in the presence of phosphate, a P_i:Fe ratio of 0.48 can be achieved (St. Pierre et al., 1988). Therefore, it is evident that more P_i can be incorporated into the core of some ferritins than is normally present. Bacterial ferritin from *Azotobacter vinlandii* has a rather high P_i:Fe ratio of 0.71 (Watt et al., 1986).

Phosphate significantly accelerates the rate of iron(II) oxidation (Figure 7) as well as the rate of disappearance of the mononuclear Fe(III)–apoferritin complex (Figure 2). The oxidation of the Fe(II) by a single-phase first-order process suggests that there is only one oxidative pathway (or possibly parallel first-order pathways). At the low levels of iron employed here, iron oxidation presumably occurs at a "ferroxidase" site on the protein. A role for both the protein and phosphate is indicated by Figure 7 (curve I) where the rate of oxidation is greatest when both are present. Futhermore, it is evident from the difference in Mössbauer parameters in Table I for samples with and without P_i present that the P_i binds to both the Fe(II) and Fe(III) in the protein samples. In the presence of P_i, the isomer shift (δ) is larger and the quadrupole splitting (Δ) is smaller for both Fe(II) and Fe(III) than when P_i is absent (Table I).

The accelerating effect of P_i on the rate of iron(II) oxidation may be due to coordination of the P_i at the protein ferroxidase site, shifting the redox potential of the iron(II) to a more negative value. Consistent with this hypothesis is the observation that the cores of bacterial ferritins have higher P_i content than mammalian ferritin and also substantially lower redox potentials (Watt et al., 1985, 1986). Alternatively, the P_i may simply facilitate iron exchange at the ferroxidase site. Whether the putative ferroxidase site suggested by this work is located on the H subunit as found for human liver ferritin (Lawson et al., 1989) is unknown.

The EPR intensities correlate with the Mössbauer spectral data when the iron(II) oxidation is carried out under the same conditions for both. Figure 3B shows that the $g' = 4.3$ Fe(III) signal reaches a maximum intensity in approximately 6–8 min at 0 °C and pH 7.5 which corresponds to the approximate time required to oxidize most of the Fe(II) in the absence of phosphate (Figure 7, curve II). This correspondence suggests that the $g' = 4.3$ signal may arise from the ferroxidase site or from a nucleation site to which the iron(II) has rapidly migrated following oxidation. The fact that the EPR spectrum at its maximum intensity accounts for only about 20% of the iron in the sample is consistent with previous Mössbauer work at 1.5–2.40 K indicating that iron(III) clusters of appreciable size are formed early in the reconstitution of ferritin with low amounts of iron (Yang et al., 1987).

The observed changes in the Fe(III) isomer shift and quadrupole splitting as the sample is progressively oxidized (Table I) indicate that the average environment of the iron(III) is being altered as the core is laid down. In the absence of P_i, the small isomer shift (δ = 0.28 mm/s) and the large quadrupole splitting (Δ = 1.22 mm/s) at 1.3 min seen early in the oxidation presumably reflect an Fe(III) coordination environment which is largely dominated by the protein. As oxidation proceeds, the isomer shift increases, and the quadrupole splitting decreases, reaching values of δ = 0.47 mm/s and Δ = 0.86 mm/s at 13.8 min at which point the iron is 90% oxidized. In the next 24 h, further reduction in the quadrupole splitting occurs to a value of 0.72 mm/s typical of the cores of native ferritins where the iron is in an environment of approximately cubic symmetry (Bauminger et al., 1980, 1989; Yang et al., 1987; Watt et al., 1985, 1986). It is evident that in the absence of phosphate continual structural rearrangement of the Fe(III), ultimately producing core, takes place in the time period following oxidation of the Fe(II). The time dependence of the Fe(III) Mössbauer parameters in Table I indicates that a similar phenomenon also takes place when phosphate is present.

The initial Fe(II) Mössbauer parameters of the protein reconstituted in the absence of phosphate (δ = 1.36 mm/s and Δ = 2.98 mm/s at 1.3 min) differ from those with buffer alone (δ = 1.39 mm/s and Δ = 3.22 mm/s) and are very similar to those reported by various groups for Fe(II) complexes of apoferritin (Jacobs et al., 1989; Bauminger et al., 1989; Yang et al., 1987). As oxidation proceeds, the parameters progressively change to δ = 1.54 mm/s and Δ = 2.66 mm/s at 6.3 min, indicating that the remaining Fe(II) has a different environment, perhaps becoming adsorbed on the surface of the hydrous ferric oxide mineral that has been generated. In contrast, the Fe(II) Mössbauer parameters of ferritin samples reconstituted in the presence of phosphate are relatively invariant with time, ranging from δ = 1.50 to 1.55 mm/s and from Δ = 2.67 to 2.60 mm/s (Table I). These values are similar to those obtained with buffer/phosphate solution alone (δ = 1.47 mm/s and Δ = 2.60 mm/s) and, within the sensitivity of the Fe(II) Mössbauer parameters, provide little evidence for a specific interaction of the bulk of the Fe(II) with the protein. However, a precipitate, presumably of $FeHPO_4$, is observed with the buffer/phosphate solution but is absent when apoferritin is present, indicating that the Fe(II) has been sequestered by the protein in some way.

ACKNOWLEDGMENTS

We thank John K. Grady for providing technical assistance, Dr. Phillip M. Hanna for helpful discussions, Dr. Andrew Laudano for assistance with the dialysis experiment, and Dr. Vincent Huyhn of Emory University for providing the Mössbauer curve-fitting program.

Registry No. Fe, 7439-89-6; PO_4^{2-}, 14265-44-2; O_2, 7782-44-7.

REFERENCES

Bauminger, E. R., Cohen, S. C., Dickson, D. P. E., Levy, A., Ofer, S., & Yariv, J. (1980) *Biochim. Biophys. Acta 623*, 237–242.

Bauminger, E. R., Harrison, P. M., Nowik, I., & Treffry, A. (1989) *Biochemistry 28*, 5486–5493.

Chasteen, N. D., & Theil, E. C. (1982) *J. Biol. Chem. 257*, 7672–7677.

Chasteen, N. D., Antanaitis, B. C., & Aisen, P. (1985) *J. Biol. Chem. 260*, 2926–2929.

Clegg, G. A., Fitton, J. E., Harrison, P. M., & Treffry, A. (1980) *Prog. Biophys. Mol. Biol. 36*, 53–86.

Devenyi, T., & Gergely, J. (1974) in *Amino Acid, Peptides and Proteins* (Devenyi, T., & Gergely, J., Eds.) pp 162–164, Elsevier Scientific Publishing Company, Amsterdam, London, and New York.

Ford, G. C., Harrison, P. M., Rice, D. W., Smith, J. M. A., Treffry, A., White, J. L., & Yariv, J. (1984) *Philos. Trans.*

R. Soc. London, B 304, 551–565.
Grady, J. K., Chasteen, N. D., & Harris, D. C. (1988) *Anal. Biochem. 173*, 111–115.
Granick, S., & Hahn, P. (1944) *J. Biol. Chem. 155*, 661–669.
Hanna, P. M., Chen, Y., & Chasteen, N. D. (1991) *J. Biol. Chem. 266*, 886–893.
Harrison, P. M. (1977) *Semin. Haematol. 14*, 598–602.
Harrison, P. M., Hoare, R. J., Hoy, T. G., & Macara, I. G. (1974) in *Iron in Biochemistry and Medicine* (Jacobs, A., & Worwood, M., Eds.) p 73, Academic Press, London.
Harrison, P. M., Treffry, A., & Lilley, T. H. (1986) *J. Inorg. Biochem. 27*, 287–293.
Heusterspreute, M., & Crichton, R. R. (1981) *FEBS Lett. 129*, 322–337.
Imai, N., Terada, H., Arata, Y., & Fujiwara, S. (1978) *Bull. Chem. Soc. Jpn. 51(9)*, 2538–2542.
Jacobs, D., Watt, G. D., Frankel, R. B., & Papaefthymiou, G. C. (1989) *Biochemistry 28*, 9216–9221.
Lawson, D. M., Treffry, A., Artymiuk, P. J., Harrison, P. M., Yewdall, S. J., Luzzago, A., Cesareni, G. Levi, S., & Arosio, P. (1989) *FEBS Lett. 254*, 207–210.
Macara, I. G., Hoy, G., & Harrison, P. M. (1972) *Biochem. J. 126*, 151.
Mann, S., Bannister, J. V., & Williams, R. J. P. (1986) *J. Mol. Biol. 188*, 225–232.
Mann, S., Williams, J. M., Treffrey, A., & Harrison, P. M. (1987) *J. Mol. Biol. 198*, 405–416.
Mansour, A. N., Thompson, C., Theil, E. C., Chasteen, N. D., & Sayers, E. E. (1985) *J. Biol. Chem. 260*, 7975.
Michaelis, L., Coryell, C. D., & Cranick, S. (1943) *J. Biol. Chem. 148*, 463–480.
Moore, G. R., Mann, S., & Bannister, J. V. (1986) *J. Inorg. Biochem. 28*, 329–336.
Rice, D. W., Ford, G. L., White, J. L., Smith, J. M. A., & Harrison, P. M. (1983) *Adv. Inorg. Biochem. 5*, 39–50.
Rohrer, J. S., Islam, Q. T., Watt, G. D., Sayers, D. E., & Theil, E. C. (1989) *J. Biol. Chem. 29*, 259–264.
Rosenberg, L. P., & Chasteen, N. D. (1982) in *Biochemistry and Physiology of Iron* (Saltman, P., & Hegenauer, J., Eds.) pp 405–407, Elsevier Biomedical, New York.
Stefanini, S., Desideri, A., Veccini, P., Drakenberg, T., & Chiancone, E. (1989) *Biochemistry 28*, 378–382.
Stookey, L. L. (1970) *Anal. Chem. 42(7)*, 779–781.
St. Pierre, T. G., Bell, S. H., Dickson, D. P. E., Mann, S., Webb, J., Moore, G. R., & Williams, R. J. P. (1986) *Biochim. Biophys. Acta 870*, 127–134.
St. Pierre, T. G., Pollard, R. K., Dickson, D. P. E., Ward, R. J., & Peters, T. J. (1988) *Biochim. Biophys. Acta 952*, 158–163.
Strickland, J. D. H., & Parsons, T. R. (1968) in *A Practical Handbook of Seawater Analysis* (Stevenson, J. C., Billingsley, L. W., & Wigmore, R. H., Eds.) pp 49–52, Queen's Printer and Controller of Stationery, Ottawa, Canada.
Theil, E. C. (1983) *Adv. Inorg. Biochem. 5*, 1–38.
Thiel, E. C. (1987) *Annu. Rev. Biochem. 56*, 289–315.
Thiel, E., (1989) *Adv. Enzymol. Relat. Areas Mol. Biol. 63*, 421–449.
Treffry, A., & Harrison, P. M. (1978) *Biochem. J. 171*, 313–320.
Treffry, A., & Harrison, P. M. (1984) *J. Inorg. Biochem. 21*, 9–20.
Treffry, A., Sowerby, J. M., & Harrison, P. M. (1979) *FEBS Lett. 100*, 33.
Wardeska, J. G., Viglione, B., & Chasteen, N. D. (1986) *J. Biol. Chem. 261*, 6677–6683.
Watt, G. D., Frankel, R. B., & Papaefthymiou, G. C. (1985) *Proc. Natl. Acad. Sci. U.S.A. 82*, 3640–3643.
Watt, G. D., Frankel, R. B., Spartalian, K., & Stiefel, E. I. (1986) *Biochemistry 25*, 4330–4336.
Webb, J., & Macey, D. J. (1983) in *Biomineralization and Biological Metal Accumulation* (Westbroek, P., & De Jong, E. W., Eds.) pp 423–427, Reidel, Dordrecht, the Netherlands.
Williams, J. M., Danson, D. P., & Janot, C. (1978) *Phys. Med. Biol. 23*, 835–851.
Yang, C.-Y., Mengher, A., Huynh, B. H., Sayers, D. E., & Theil, E. C. (1987) *Biochemistry 26*, 497–503.